

Studying the Performance of the Jellyfish Search Optimiser for the Application of Projection Pursuit

H. Sherry Zhang^{a,*}, Dianne Cook^b, Nicolas Langrené^c, Jessica Wai Yin Leung^b

^a*University of Texas at Austin, Department of Statistics and Data Sciences, Austin, United States, 78751*

^b*Monash University, Department of Econometrics and Business Statistics, Melbourne, Australia, 3800*

^c*Guangdong Provincial Key Laboratory of Interdisciplinary Research and Application for Data Science, BNU-HKBU United International College, Department of Mathematical Sciences, Zhuhai, China, 519087*

Abstract

The projection pursuit (PP) guided tour interactively optimises a criteria function known as the PP index, to explore high-dimensional data by revealing interesting projections. The optimisation in PP can be non-trivial, involving non-smooth functions and optima with a small “squint angle”, detectable only from close proximity. To address these challenges, this study investigates the performance of a recently introduced swarm-based algorithm, Jellyfish Search Optimiser (JSO), for optimising PP indexes. The performance of JSO for visualising data is evaluated across various hyper-parameter settings and compared with existing optimisers. Additionally, this work proposes novel methods to quantify two properties of the PP index – smoothness and squintability – that capture the complexities inherent in PP optimisation problems. These two metrics are evaluated along with JSO hyper-parameters to determine their effects on JSO success rate. Our numerical results confirm the positive impact of these metrics on the JSO success rate, with squintability being the most significant. The JSO algorithm has been implemented in the `tourr` package and functions to calculate smoothness and squintability are available in the `ferrn` package.

Keywords: projection pursuit, jellyfish search optimiser (JSO), optimisation, grand tour, high-dimensional data, exploratory data analysis

1. Introduction

Projection Pursuit (PP) (Kruskal [1], Friedman and Tukey [2]) is a dimension reduction technique aimed at identifying informative linear projections of data. The method involves optimising an objective function known as the PP index (e.g. Hall [3], Cook et al. [4], Lee and Cook [5], Loperfido [6], Loperfido [7]), which defines the criteria for what constitutes interesting or informative projections. Let $X \in \mathbb{R}^{n \times p}$ be the data matrix, $A \in \mathbb{R}^{p \times d}$ be an orthonormal matrix, where A belongs to the Stiefel manifold $\mathcal{A} = V_d(\mathbb{R}^p)$. The projection $Y = XA$ is a linear transformation that maps data from a p -dimensional space into a d -dimensional space. The index function $f(XA) : \mathbb{R}^{n \times d} \rightarrow \mathbb{R}$ is a scalar function that measures an interesting aspect of the projected data, such as deviation from normality, presence of clusters, non-linear structure, or other features of interest. For a fixed data, PP finds the orthonormal basis A that maximises the index value of the projection, $Y = XA$:

*Corresponding author

Email addresses: huize.zhang@austin.utexas.edu (H. Sherry Zhang), dcook@monash.edu (Dianne Cook), nicolaslangrene@uic.edu.cn (Nicolas Langrené), Jessica.Leung@monash.edu (Jessica Wai Yin Leung)

$$\max_{A \in \mathcal{A}} f(XA) \quad \text{subject to} \quad A'A = I_d \quad (1)$$

The index functions can be non-linear and non-convex, hence an effective and efficient optimisation procedure is essential to explore the data landscape and achieve a globally optimal viewpoint of the data.

Optimisation of PP is typically investigated in the literature when new indexes are proposed [8, 9, 10] or when visualisation method are used to track the optimisation process. Cook et al. [11] introduced the PP guided tour, which monitors the optimisation visually to see the data projections leading in and out of the optima. An implementation is available in the `tourrr` package [12] in R [13]. Zhang et al. [14] illustrated how to diagnose optimisation processes, particularly focusing on the guided tour, and revealed a need for improved optimisation. While improving the quality of the optimisation solutions in the tour is essential, it is also important to be able to view the data projections as the optimisation progresses. Integrating the guided tour with a global optimisation algorithm that is efficient in finding the global optimal and enables viewing of the projected data during the exploration process is a goal.

Here, the potential for a Jellyfish Search Optimiser (JSO) to be integrated with the projection pursuit guided tour is explored. JSO, [15] - [16], inspired by the search behaviour of jellyfish in the ocean, is a swarm-based metaheuristic designed to solve global optimisation problems. Compared to traditional methods, JSO has demonstrated stronger search ability and faster convergence, and requires fewer tuning parameters. These practical advantages make JSO a promising candidate for enhancing PP optimisation.

The primary goal of the study reported here is to investigate the performance of JSO in PP optimisation for the guided tour. It is of interest to assess how quickly and closely the optimiser reaches a global optima, for various PP indexes that may have differing complexities. To observe the performance of JSO with different types of PP indexes, metrics are introduced to capture specific properties of the index including squintability (based on Tukey and Tukey [17]'s squint angle) and smoothness as introduced in Laa and Cook [18]. Here we mathematically define metrics for squintability and smoothness, which is new for the field. A series of simulation experiments using various datasets and PP indexes are conducted to assess JSO's behaviour and its sensitivity to hyper-parameter choices (number of jellyfish and maximum number of tries). The relationship between the JSO performance, hyper-parameter choices and properties of PP indexes (smoothness and squintability) is analysed to provide guidance on selecting optimisers for practitioners using projection pursuit. Additionally, it aims to guide the design of new indexes that facilitate easy optimization for PP researchers.

The paper is structured as follows. Section 2 introduces the background of PP guided tour and reviews existing optimisers and index functions in the literature. Section 3 details JSO and introduces metrics that measure different properties of PP indexes, smoothness and squintability. Section 4 details two simulation experiments to assess JSO's performance: one comparing JSO's performance improvements relative to an existing optimiser, Creeping Random Search (CRS), and the other studying the impact of different PP index properties on optimisation performance. Section 5 presents the results. Section 6 summarises the work and provides suggestions for future directions.

2. Projection pursuit, tours, index functions and optimisation

A tour on high-dimensional data is constructed by geodesically interpolating between pairs of planes. Any plane is described by an orthonormal basis, A_t , where t represents time in the sequence. The term “geodesic” refers to maintaining the orthonormality constraint so that each view shown is correctly a projection of the data. The PP guided tour operates by geodesically interpolating to target planes (projections) which have high PP index values, as provided by the optimiser. The geodesic interpolation means that the viewer sees a continuous sequence of projections of the data, so they can watch patterns of interest forming as the function is optimised. There are five (unsophisticated) optimisation methods implemented in the `tourrr` package:

- `search_geodesic()`: provides a pseudo-derivative optimisation. It searches locally for the best direction, based on differencing the index values for very close projections. Then it follows the direction along the geodesic path between planes, stopping when the next index value fails to increase.
- `search_better()`: also known as Creeping Random Search (CRS), is a brute-force optimisation searching randomly for projections with higher index values.
- `search_better_random()`: is essentially simulated annealing [19] where the search space is reduced as the optimisation progresses.
- `search_posse()`: implements the algorithm described in Posse [20].
- `search_polish()`: is a very localised search, to take tiny steps to get closer to the local maximum.

There are several PP index functions available: `holes()` and `cmass()` [4]; `lda_pp()` [21]; `pda_pp()` [5]; `dcor2d()` and `splines2d()` [22]; `norm_bin()` and `norm_kol()` [23]; `slice_index()` [24]. Most are relatively simply defined, for any projection dimension, and implemented because they are relatively easy to optimise. A goal is to be able to incorporate more complex PP indexes, for example, based on scagnostics (Wilkinson et al. [25], Wilkinson and Wills [26]).

An initial investigation of PP indexes, and the potential for scagnostics is described in Laa and Cook [18]. To be useful here an optimiser needs to be able to handle index functions which are possibly not very smooth. In addition, because data structures might be relatively fine, the optimiser needs to be able to find maxima that occur with a small squint angle, that can only be seen from very close by. One last aspect that is useful is for an optimiser to return local maxima in addition to global because data can contain many different and interesting features.

3. The jellyfish optimiser and properties of PP indexes

JSO mimics the natural movements of jellyfish, which include passive and active motions driven by ocean currents and their swimming patterns, respectively. In the context of optimization, these movements are abstracted to explore the search space, aiming to balance exploration (searching new areas) and exploitation (focusing on promising areas). The algorithm aims to find the optimal solution by adapting the behaviour of jellyfish to navigate towards the best solution over iterations [15].

To solve the optimisation problem embedded in the PP guided tour, a starting projection, an index function, the number of jellyfish, and the maximum number of trials (tries) are provided as input. Then, the current projection is evaluated by the index function. The projection is then moved in a direction determined by a random factor, influenced by how far along we are in the optimisation process. Occasionally, completely new directions may be taken like a jellyfish might with ocean currents. A new projection is accepted if it is an improvement compared to the current one, rejected otherwise. This process continues and iteratively improves the projection, until the pre-specified maximum number of trials is reached.

Algorithm: Jellyfish Optimizer Pseudo Code

```

Input: current_projections, index_function, trial_id, max_trial
Output: optimised_projection
Initialize current_best as the projection with the best index value from current_projections, and
current_idx as the array of index values for each projection in current_projections
for each trial_id in 1 to max_tries do
    Calculate the time control value,  $c_t$ , based on current_idx and max_trial
    if  $c_t$  is greater than or equal to 0.5 then
        Define trend based on the current_best and current_projections
        Update each projection towards the trend using a random factor and orthonor-
        malisation
    else

```

```

if a random number is greater than  $1 - c_t$  then
    Slightly adjust each projection with a small random factor (passive)
else
    For each projection, compare with a random jellyfish and adjust towards
    or away from it (active)
Update the orientation of each projection to maintain consistency
Evaluate the new projections using the index function
if any new projection is worse than the current, revert to the current_projections for
that case
    Determine the projection with the best index value as the new current_best
if trial_id  $\geq$  max_trial, print the last best projection exit
return the set of projections with the updated current_best as the optimised_projection

```

The JSO implementation involves several key parameters that control its search process in optimization problems. These parameters are designed to guide the exploration and exploitation phases of the algorithm. While the specific implementation details can vary depending on the version of the algorithm or its application, the focus is on two main parameters that are most relevant to our application: the number of jellyfish and the maximum number of tries.

Laa and Cook [18] has proposed five criteria for assessing projection pursuit indexes (smoothness, squintability, flexibility, rotation invariance, and speed). Since not all index properties affect the optimisation process, the focus here is on the first two properties, *smoothness* (Section 3.1) and *squintability* (Section 3.2), for which metrics are proposed to quantify them.

3.1. Smoothness

This subsection proposes a metric for the smoothness of a projection pursuit index.

A classical way to describe the smoothness of a function is to identify how many continuous derivatives of the function exist. This can be characterized by Sobolev spaces [27].

Definition 1. *The Sobolev space $W^{k,p}(\mathbb{R})$ for $1 \leq p \leq \infty$ is the set of all functions f in $L^p(\mathbb{R})$ for which all weak derivatives $f^{(\ell)}$ of order $\ell \leq k$ exist and have a finite L^p norm.*

The Sobolev index k in Definition 1 can be used to characterize the smoothness of a function: if $f \in W^{k,p}$, then the higher k , the smoother f . While this Sobolev index k is a useful measure of smoothness, it can be difficult to compute or even estimate in practice.

To obtain a computable estimator of the smoothness of the index function f , we propose an approach based on random fields. If a PP index function f is evaluated at some random bases, as is done at the initialization stage of JSO, then these random index values can be interpreted as a random field, indexed by a space parameter, namely the random projection basis. This analogy suggests to use this random training sample to fit a spatial model. We propose to use a Gaussian process equipped with a Matérn covariance function, due to the connections between this model and Sobolev spaces, see for example Porcu et al. [28].

The distribution of a Gaussian process is fully determined by its mean and covariance function. The smoothness property comes into play in the definition of the covariance function: if a PP index is very smooth, then two close projection bases should produce close index values (strong correlation); by contrast, if a PP index is not very smooth, then two close projection bases might give very different index values (fast decay of correlations with respect to distance between bases). Popular covariance functions are parametric positive semi-definite functions. In particular, the Matérn class of covariance functions has a dedicated parameter to capture the smoothness of the Gaussian field.

Definition 2. The Matérn covariance function K is defined by

$$K(u) = K_{\nu, \eta, \ell}(u) := \eta^2 \frac{(\sqrt{2\nu} \frac{u}{\ell})^\nu}{\Gamma(\nu) 2^{\nu-1}} \mathcal{K}_\nu \left(\sqrt{2\nu} \frac{u}{\ell} \right), u \geq 0 \quad (2)$$

where $\nu > 0$ is the smoothness parameter, η is the outputscale, ℓ is the lengthscale, and \mathcal{K}_ν is the modified Bessel function [29, 10.25]. A multivariate extension $K(u)$, $u \in \mathbb{R}^d$ can be obtained by products of univariate covariance functions (2).

The Matérn covariance function can be expressed analytically when ν is a half-integer, the most popular values in the literature being $\frac{1}{2}$, $\frac{3}{2}$ and $\frac{5}{2}$ [30]. The parameter ν , called *smoothness parameter*, controls the decay of the covariance function. As such, it is an appropriate measure of smoothness of a random field, as shown by the simulations on Figure 1 and Figure 2. For example, Karvonen [31] showed that if a function f has a Sobolev index of k , then the smoothness parameter estimate ν in (2) cannot be asymptotically less than k . See the survey Porcu et al. [28] for additional results on the connection between the Matérn model and Sobolev spaces. An interesting result is that the asymptotic case $\nu \rightarrow \infty$ coincides with the Gaussian kernel: $K_\infty(u) = \exp(-u^2/2)$.

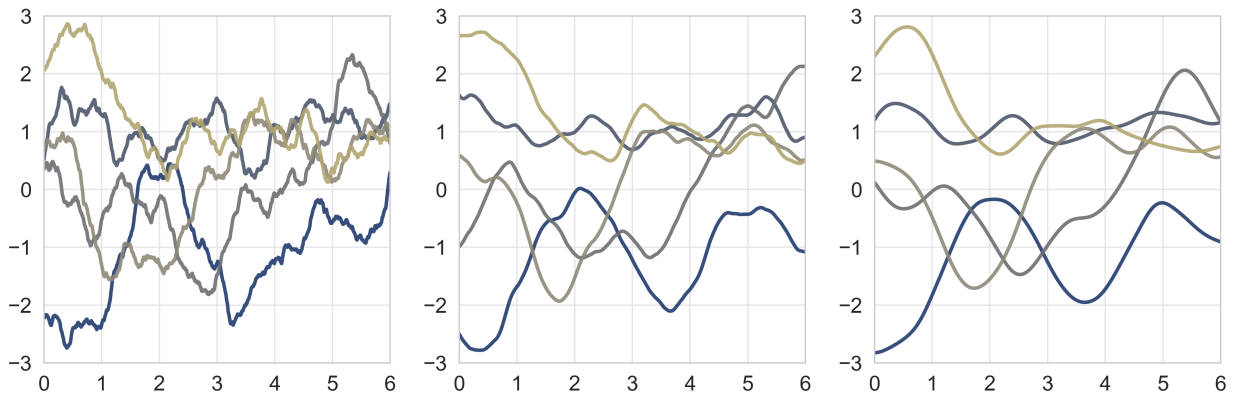


Figure 1: Five random simulations from a Gaussian Process defined on \mathbb{R} with zero mean and Matérn- ν covariance function, with $\nu = 1$ (left), $\nu = 2$ (middle), and $\nu = 4$ (right), showing that higher values of ν produce smoother curves.

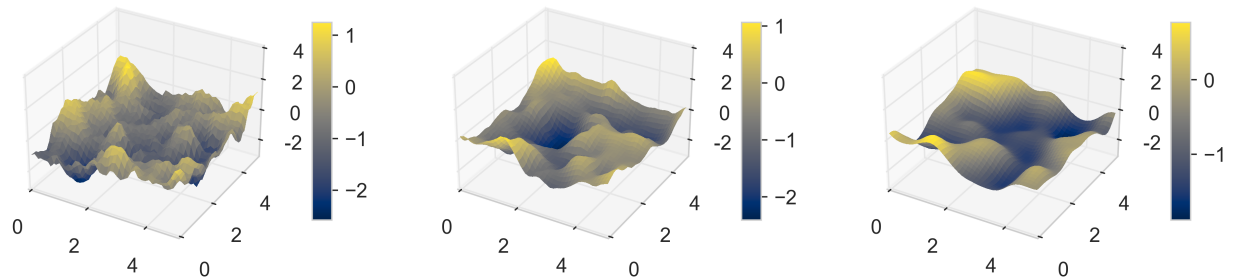


Figure 2: One random simulation from a Gaussian Process defined on \mathbb{R}^2 with zero mean and Matérn- ν covariance function, with $\nu = 1$ (left), $\nu = 2$ (middle), and $\nu = 4$ (right), showing that higher values of ν produce smoother surfaces.

In view of these results, the parameter ν is suggested as a measure of the smoothness of the PP index function by fitting a Gaussian process prior with Matérn covariance on a dataset generated by random evaluations of the index function, as done at the initialization stage of the jellyfish search optimization. There exist several R packages, such as GpGp [32] or ExaGeoStatR [33], to fit the hyperparameters of a GP

covariance function on data, which is usually done by maximum likelihood estimation. In this project, the `GpGp` package is used.

Definition 3. Let $\mathbf{A} = [A_1, \dots, A_N] \in (\mathbf{R}^{p \times d})^N$ be d -dimensional projection bases, let $\mathbf{y} = [f(XA_1), \dots, f(XA_N)]$ be the corresponding PP index values, and let $\mathbf{K} = [K_\theta(A_i, A_j)]_{1 \leq i, j \leq N} \in \mathbf{R}^{N \times N}$ be the Matérn covariance matrix evaluated at the input bases, where the vector θ contains all the parameters of the multivariate Matérn covariance function K (smoothness, outputscale, lengthscales). The log-likelihood of the parameters θ is defined by

$$\mathcal{L}(\theta) = \log p(\mathbf{y} | \mathbf{A}, \theta) = -\frac{1}{2}\mathbf{y}^\top(\mathbf{K} + \sigma^2\mathbf{I})^{-1}\mathbf{y} - \frac{1}{2}\log(\det(\mathbf{K} + \sigma^2\mathbf{I})) - \frac{N}{2}\log(2\pi). \quad (3)$$

where the nugget parameter σ is the standard deviation of the intrinsic noise of the Gaussian process. The optimal parameters (including smoothness) are obtained by maximum log-likelihood

$$\theta^* = \max_{\theta} \mathcal{L}(\theta) \quad (4)$$

The resulting optimal smoothness parameter ν is chosen as our smoothness metric.

The value of the optimal smoothness parameter $\nu > 0$ can be naturally interpreted as follows: the higher ν , the smoother the index function.

3.2. Squintability

Here the formal definition of projection distance and squint angle are given, before the definition of squintability. Two approaches to compute this metric numerically, are described.

Definition 4 (projection distance). Recall that $A \in \mathbf{R}^{p \times d}$ is a d -dimensional orthonormal matrix. Let A^* be the optimal matrix that achieves the maximum index value for a given data. The projection distance $d(A, A^*)$ between A and A^* is defined as $d(A, A^*) = \|AA' - A^*A^{*\prime}\|_F$ where $\|\cdot\|_F$ denotes the Frobenius norm, given by $\|M\|_F = \sqrt{\sum_{ij} M_{ij}^2}$.

Definition 5 (squint angle). Let A and B be two d -dimensional orthonormal matrices in \mathbf{R}^p . The squint angle θ between the subspace spanned by A and B is defined as the smallest principal angle between these subspaces: $\theta = \min_{i \in \{1, \dots, d\}} \arccos(\tau_i)$, where τ_i are the singular values of the matrix $M = A^T B$ obtained from its singular value decomposition.

Squintability can be defined as how the index value $f(XA)$ changes with respect to the projection distance $d(A, A^*)$, over the course of the JSO:

Definition 6 (squintability). Let $g : \mathbb{R} \mapsto \mathbb{R}$ be a decreasing function that maps the projection distance $d(A, A^*)$ to the index value $f(XA)$, such that $g(d(A, A^*)) = f(XA)$. For brevity, denote $g(d)$ as $g(d(A, A^*))$. The squintability of an index function $f(XA)$ is defined as

$$\varsigma(f) = -c \times \max_d g'(d) \times \arg \max_d g'(d) \quad (5)$$

where c is a constant scaling factor, $-\max_d g'(d)$ represents the largest gradient of $-g$ and $\arg \max_d g'(d)$ represents the projection distance at which this largest gradient is attained.

It is expected that these two values should be both high in the case of high squintability (fast increase in f early on), and both low in the case of low squintability (any substantial increase in f happens very late, close to the optimal angle). This suggests that their product (5) should provide a sensible measure of squintability. The multiplicative constant 4, which can be deemed arbitrary, does not change the interpretation of the squintability metric ς ; it is here to adjust the range of values of ς and simplify the explicit formula for ς obtained later on.

From the definition, the following proposition can be derived:

Proposition 1. Let $g_1(d)$ be a convex function and $g_2(d)$ be a concave function, where $d \in [0, D]$ and $g_1(d), g_2(d) \in [0, 1]$. Assume both functions achieve the same maximum gradient, i.e., $\max g'_1(d_1) = \max g'_2(d_2) = -g_{\max}$, it follows that $d_1 < d_2$ and $\varsigma(f_1) < \varsigma(f_2)$.

From Tukey and Tukey [17] and Laa and Cook [18], a large squint angle implies that the objective function value is close to optimal even when the perfect view to see the structure is far away. A small squint angle means that the PP index value improves substantially only when the perfect view is close by. As such, low squintability implies rapid improvement in the index value when near the perfect view. For PP, a small squint angle is considered to be undesirable because it means that the optimiser needs to be very close to be able to “see” the optima. Thus, it could be difficult for the optimiser to find the optima. The mathematical formulation of this intuition is proposed below:

It is expected that for a PP index with high squint angle, the optimization (1) should make substantial progress early on. Conversely, for a PP index with low squint angle, it might take a long while for the optimization to make substantial progress, as the candidate projections would need to be very close to the optimal one for the structure of the index function to be visible enough to be amenable to efficient optimization. This observation suggests that the extreme values of f' (the ones for which $f'' = 0$, assuming that f is twice differentiable), and the projection distances for which these values are attained, are crucial in the mathematical definition of squintability.

To compute the squintability metric (5) in practice, several approaches are possible. The first one is to propose a parametric model for f , and use it to obtain an explicit formula for ς . Numerical experiments suggest a scaled sigmoid shape as described below. Define

$$\ell(x) := \frac{1}{1 + \exp(\theta_3(x - \theta_2))} , \quad (6)$$

which is a decreasing logistic function depending on two parameters θ_2 and θ_3 , such that $\ell(\theta_2) = \frac{1}{2}$. Then, define

$$f(x) = (\theta_1 - \theta_4) \frac{\ell(x) - \ell(x_{\max})}{\ell(0) - \ell(x_{\max})} + \theta_4 , \quad (7)$$

which depends on three additional parameters, θ_1 , θ_2 , and x_{\max} , such that $f(0) = \theta_1$ and $f(x_{\max}) = \theta_4$. Under the parametric model (7), the squintability metric (5) can be shown to be equal to

$$\varsigma = \frac{(\theta_1 - \theta_4)\theta_2\theta_3}{\ell(0) - \ell(x_{\max})} . \quad (8)$$

In practice, the parameters of this model (7) can be estimated numerically, for example by non-linear least squares, and then used to evaluate ς as in equation (8).

Alternatively, one can estimate (5) in a nonparametric way, for example by fitting f using kernel regression, then numerically estimate the angle at which $-f'$ attains its highest value.

4. Simulation details

The JSO performance is compared with an existing optimiser, Creeping Random Search (CRS) [14, 18] used in the PP guided tour to explore JSO’s behaviour under different hyper-parameter and data dimension combinations. The second simulation studies the effect of index properties (smoothness and squintability), along with JSO hyper-parameters, and data dimension, on the success rate of the JSO performance. This section describes the simulation details, with the results deferred to Section Section 5.

4.1. Performance of JSO relative to CRS

The performance of JSO is investigated both in comparison to the existing optimizer, CRS, and across various hyper-parameter values. The performance is measured by the success rate, defined as the proportion of simulations that achieves a final index value within 0.05 of the best index value found among all 50 simulations (see Figure 3 for an illustration). This comparison is based on projection pursuit to find the pipe shape investigated by Laa and Cook [18] using the **holes** index.

Fifty simulations are conducted with both JSO and CRS, in four different data dimensions ($d = 6, 8, 10, 12$). JSO uses 100 jellyfishes with a maximum of 100 tries, while the CRS allows a maximum of 1000 samples at each iteration before the algorithm terminates. The different numbers account for the multiple paths of JSO to enable fairer comparison with CRS. The results of the simulation are collected using the data structure proposed in Zhang et al. [14] for assessing JSO, where the design parameters are stored along with index value, projection basis, random seed, and computation time.

Fifty additional simulations are conducted for each hyper-parameter combination to analyze how they affect the JSO success rate. This includes variations in the number of jellyfish (20, 50, and 100) and the maximum number of tries (50 and 100).

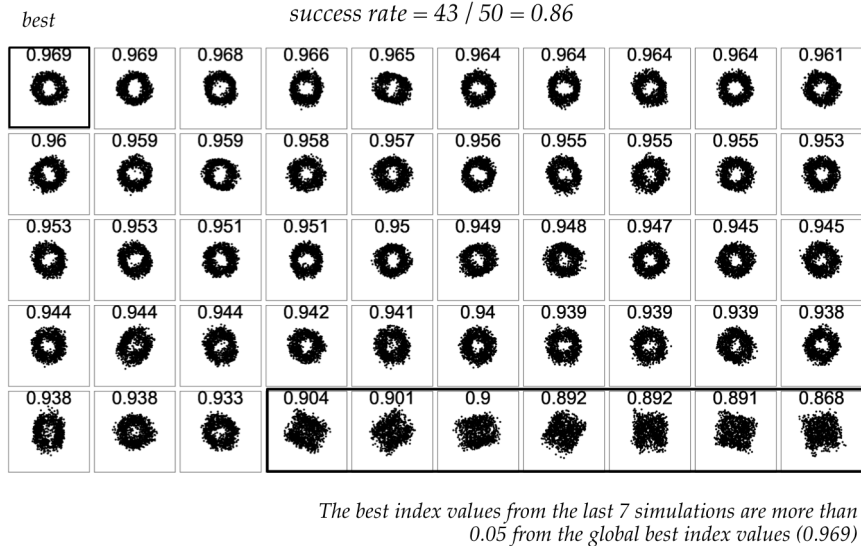


Figure 3: Illustration of success rate calculation: Final projections based on projection pursuit to find the pipe shape in 8D data using the holes index, optimised by CRS, in 50 simulations. The 50 final projections are sorted by their index values. The highest index value found across all simulations is 0.969. Out of the 50 simulations, 43 achieved an index value within 0.05 of the best, resulting in a success rate of 0.86 (43/50).

4.2. Factors affecting JSO success rate: index properties and jellyfish hyper-parameters

To assess JSO's performance across various scenarios, two different data shapes, pipe and a sine wave, are investigated in 6D and 8D spaces using six different PP indexes: **dcor2d_2**, **loess2d**, **MIC**, **TIC**, **spline**, and **stringy**, with varied JSO hyper-parameters. A total of 52 combinations result, comprising of 24 computed on the pipe data and 28 on the sine-wave data. Again, JSO is run 50 times to calculate the success rate for each projection pursuit.

Smoothness and squintability are computed following the procedures outlined in Section 3.1 and Section 3.2 and as illustrated in Figure 4 and Figure 5.

To compute smoothness, 300 random bases are simulated. Index values and projection distance (to the optimal basis) are calculated for each random basis before fitting the Gaussian process model to obtain the smoothness measure for the index.

To compute squintability, 50 random bases are sampled and interpolated to the optimal basis with a step size of 0.005. Index values and projection distances are calculated for these interpolated bases and the index values are averaged with a bin width of 0.005. A four-parameter scaled logistic function is fitted to the index values against projection distances, estimated by non-linear least squares. The squintability measure is then calculated as (8).

To construct a relationship among success rate, index properties (smoothness and squintability), and jellyfish hyper-parameters, a generalised linear model is fitted using a binomial family and a logit link function. The data is pre-processed by 1) scaling the JSO hyper-parameters by a factor of 10 for interpretation, 2) creating a new binary variable `long_time` to indicate cases with an average run time over 30 seconds, and 3) re-coding the success rate for the `stringy` index as 0, because none of the 50 simulations correctly identified the sine-wave shape.

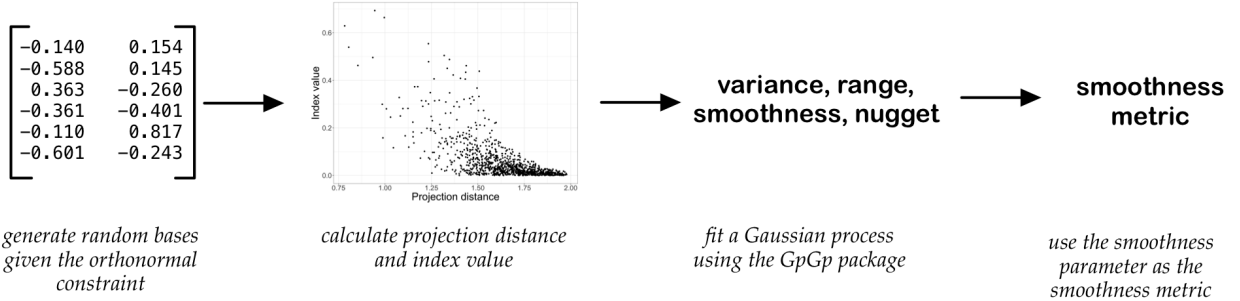


Figure 4: Illustration of steps to calculate smoothness. For a given projection pursuit problem defined by the shape to find, data dimension and the index function, 1) sample random bases given the orthonormality constraint, 2) calculate the projection distance and the index value for each random basis, and 3) fit a Gaussian process model of index values against projection distances to obtain the smoothness measure.

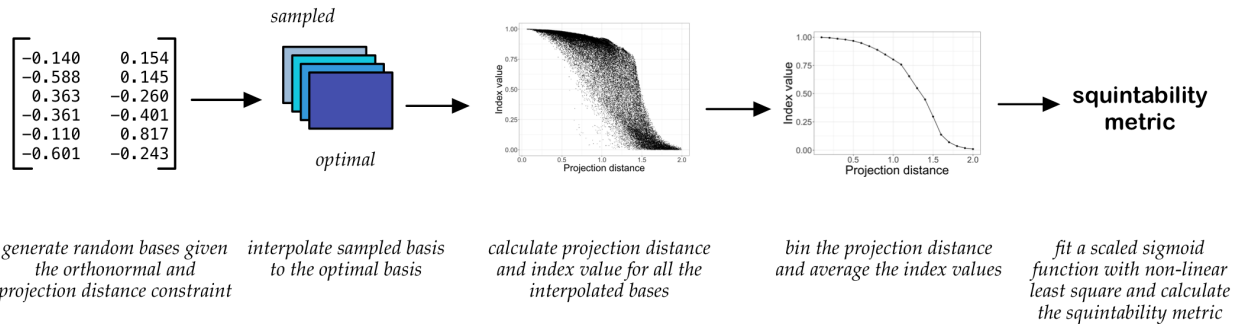


Figure 5: Illustration of steps to calculate squintability. For a given projection pursuit problem defined by the shape to find, data dimension and the index function, 1) sample random bases given the orthonormality and projection distance constraint, 2) interpolate the sampled bases to the optimal basis and calculate the projection distance and the index value for each interpolated basis. 3) bin the index values by projection distances to obtain the average index value for each bin, 4) fit the scaled sigmoid function in equation (5) to the binned index values against projection distances using non-linear least square, 5) calculate the squintability measure using equation (8) with parameters estimated from the model.

5. Results

The results from the first simulation described in Section 4 are analysed based on the final projections across two optimisers (JSO and CRS) and the success rate across JSO hyper-parameters. In the second simulation, smoothness and squintability are calculated across a collection of pipe-finding and sine-wave finding problems to construct the relationship between success rate, JSO hyper-parameters, and index properties.

The final projections found by the two optimisers (JSO and CRS) are presented in Figure 6, broken down by 10th quantile, faceted by the data dimensions. In the 6-dimensional data scenario, JSO consistently identifies a clear pipe shape. The CRS also finds the pipe shape but with a wide rim, suggesting a further polish search may be required. With increasing dimensions, JSO may not always identify the pipe shape due to random sampling, but it still finds the pipe shape in over 50% of cases. Compared to CRS, JSO achieves higher index values and clearer pipe shapes across all quantiles in data of 8, 10, 12 dimensions, suggesting its advantage in exploring high-dimensional spaces.

The success rate calculated at each hyper-parameter combination (number of jellyfish and the maximum number of tries) is presented in Figure 7. As the number of jellyfish and maximum tries increase, the success rate also increases. For simpler problems (6 dimensions), small parameter values (20 jellyfishes and a maximum of 50 tries) can already achieve a high success rate. However, larger parameter values (i.e. 100 jellyfishes and a maximum of 100 tries) are necessary for higher-dimensional problems (8, 10, and 12 dimensions). Increasing both parameters enhances the performance of JSO, but it also extends the computational time required for the optimisation, which can be computationally intensive when evaluating the index function (such as scagnostic indexes) multiple times across numerous iterations.

The index properties, including smoothness and squintability, offer numerical metrics to characterise the complexity of projection pursuit optimisation problems. Table 1 presents the parameters for calculating both metrics estimated from the Gaussian process (variance, range, smooth, and nugget) and the scaled logistic function (θ_1 to θ_4) for each case considered in the simulation. The column “smooth” is used as the smoothness metric and the column “squint” is calculated as equation (8) as the squintability metric. Table 3 presents the results of fitting a generalised linear model with a binomial family and a logit link function to a sample of data in Table 2, where all the three components (success rate, JS hyper-parameters, and index properties) are combined. The model suggests that JSO success rate is positively associated with the two hyper-parameters, as well as with the index properties: smoothness and squintability. Specifically, using 10 more jellyfish and 10 more tries increases the odd ratio of success by 24.11% and 11.93%, respectively. However, being flagged with long runtime and an increase of data dimension reduce the success rate by 41.72% and 53.36%, respectively. The variable **squintability** and **dimension** are significant, suggesting their importance relative to JSO hyper-parameters in the optimisation success. In defining a projection pursuit problem, factors such as the shape-to-find, the index function used, and the data dimension, determine the properties such as smoothness and squintability. These metrics can then be compared across different problems to understand their relative complexities. The results suggest that squintability has a more significant influence than smoothness on the success rate of JSO. Once the characteristics of the projection pursuit problem are fully understood, increasing JSO hyper-parameters can enhance the search effectiveness, however, it is also important to consider the resulting increase in computational complexity.

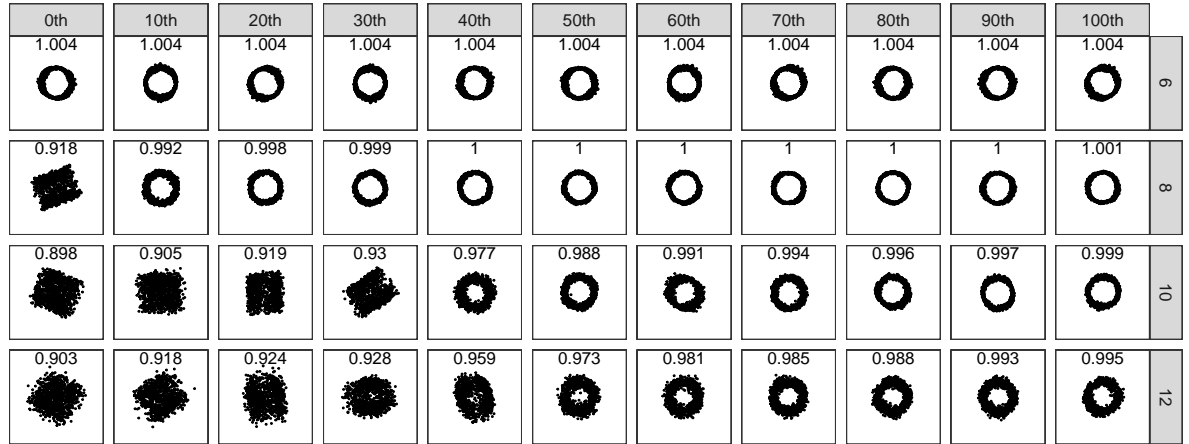
6. Conclusion

This paper has presented new metrics to mathematically define desirable features of PP indexes, squintability and smoothness, and used these to assess the performance of the new jellyfish search optimiser. The metrics will be generally useful for characterising PP indexes, and help with developing new indexes.

In the comparison of the JSO against the currently used CRS, as expected the JSO vastly out-performs CRS, and provides a high probability of finding the global optima. The JSO obtains the maximum more cleanly, with a slightly higher index value, and plot of the projected data showing the structure more clearly.

The JSO performance is affected by the hyper-parameters, with a higher chance of reaching the global optima when more jellyfish are used and the maximum number of tries is increased. However, it comes at a computational cost, as expected. The performance declines if the projection dimension increases and if the PP index has low squintability. The higher the squintability the better chance the JSO can find the optima. However, interestingly smoothness does not affect the JSO performance.

a. JSO



b. CRS

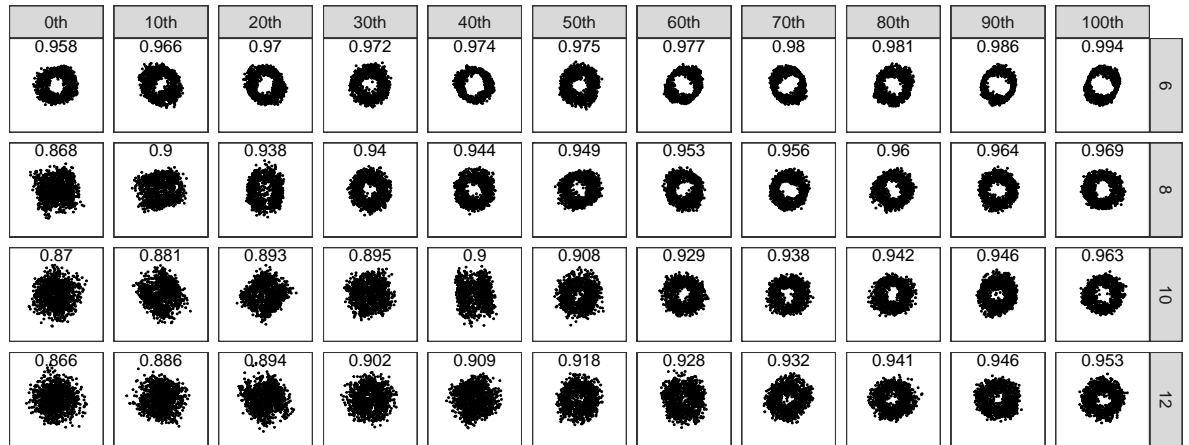


Figure 6: Projections found by the JSO and CRS at each 10th quantile across 50 simulations. The projection pursuit problem is to find the pipe shape using the holes index in the 6, 8, 10, and 12-dimensional spaces. The JSO uses 100 jellyfishes and a maximum number of tries of 100. The CRS uses a maximum of 1000 tries in each step of random sampling step before the algorithm terminates. In the 6-D data space, JSO always finds a clear pipe shape while the CRS also finds the pipe shape but with a wide rim. At higher data dimensions, JSO finds a higher index value and a clearer pipe shape across all the quantiles than the CRS

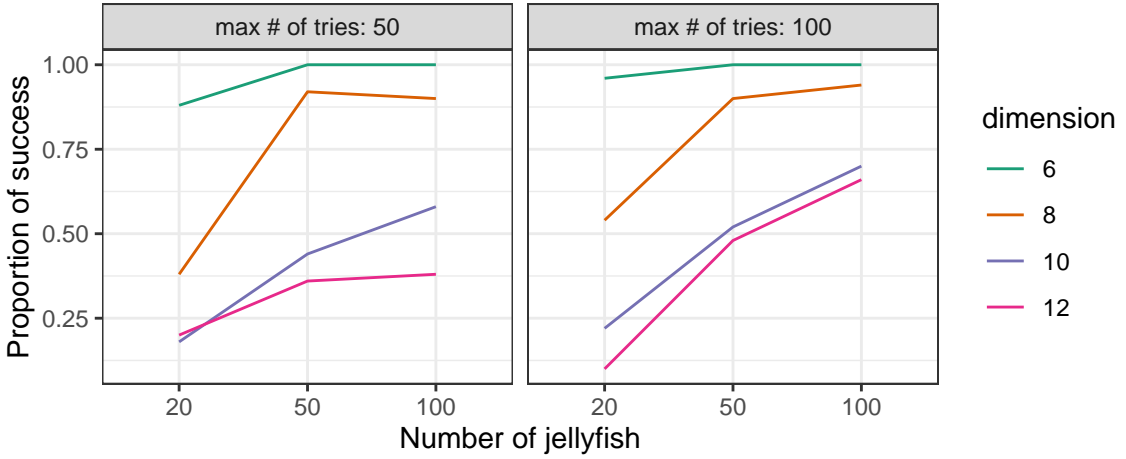


Figure 7: Proportion of simulations reaches near-optimal index values in the pipe-finding problem using the holes index. The proportion is calculated based on the number of simulations, out of 50, that achieve an index value within 0.05 of the best-performing simulation. As the dimensionality increases, the proportion of simulations reaching the optimal index value increases.

Table 1: Parameters estimated from the Gaussian process (including variance, range, smoothness, and nugget) and scaled logistic function (θ_1 to θ_4) for the pipe-finding and sine-wave finding problems. The column “smooth” and “squint” represent the smoothness and squintability measures.

	shape	index	d	variance	range	smooth	nugget	θ_1	θ_2	θ_3	θ_4	squint
1	pipe	holes	6	0.00	0.37	2.36	0.22	1.02	0.86	3.37	0.02	3.05
2	pipe	holes	8	0.00	0.18	2.19	0.82	1.01	0.87	3.26	0.03	2.96
3	pipe	holes	10	0.00	0.11	2.19	3.03	1.02	0.88	3.15	0.02	2.95
4	pipe	holes	12	0.00	0.15	2.29	1.58	1.01	0.88	3.34	0.00	3.12
5	sine	MIC	6	0.02	0.09	2.46	0.08	0.89	0.57	1.62	-0.02	1.26
6	sine	MIC	8	0.02	0.08	2.64	0.08	0.93	0.33	1.31	-0.03	0.77
7	sine	TIC	6	0.12	0.11	2.44	0.09	0.95	0.54	1.72	-0.03	1.32
8	sine	TIC	8	0.12	0.10	2.47	0.09	0.95	0.56	1.72	-0.03	1.37
9	sine	dcor2d	6	0.03	0.17	2.66	0.11	0.95	1.04	2.74	-0.02	2.95
10	sine	loess2d	6	0.08	0.34	1.99	0.31	1.02	1.04	2.65	0.08	2.76
11	sine	splines2d	6	0.04	0.24	2.54	0.10	1.01	1.05	2.73	-0.01	3.12
12	sine	stringy	6	0.00	0.01	1.54	38.17	1.05	0.01	254.73	0.05	2.96

Table 2: The first 7 rows of the datasets processed for modelling.

index	d	smoothness	squintability	n. jellyfish	max. tries	success rate	time (sec)
MIC	6	2.46	1.26	20	50	0.12	2.48
MIC	6	2.46	1.26	20	100	0.24	8.95
MIC	6	2.46	1.26	50	50	0.52	5.65
MIC	6	2.46	1.26	50	100	0.64	13.22
MIC	6	2.46	1.26	100	50	0.76	19.45
MIC	8	2.64	0.77	20	50	0.08	2.57
MIC	8	2.64	0.77	20	100	0.08	4.96

Table 3: Model estimates of proportion of jellyfish success on index properties and jellyfish hyper-parameters from the generalised linear model with a binomial family and a logit link function. The variable smoothness, squintability, number of jellyfish and maximum number of tries are positively associated with JSO success rate while data dimension and being flagged as long runtime are negatively associated with the success rate. The variable squintability and dimension are significant, suggesting their importance relative to jellyfish hyper-parameters in the optimisation success.

term	estimate	std.error	statistic	p.value
Intercept	-4.52	5.33	-0.85	0.40
Smoothness	1.19	1.92	0.62	0.53
Squintability	2.06	0.68	3.01	0.00
Dimension (d)	-0.63	0.26	-2.46	0.01
Long time	-0.87	1.29	-0.68	0.50
N. jellyfish	0.22	0.13	1.70	0.09
Max. tries	0.11	0.15	0.75	0.45

The new JSO is integrated with the current implementation of the projection pursuit guided tour in the `tourrr` package, and can be further examined using PP optimisation diagnostics in the `ferrn` package. Using the JSO is a little different than the current CRS, because it runs many paths. The recommended approach is to conduct the optimisation off-line, extract the bases of a selected jellyfish, and then use the planned tour to follow selected jellyfish. The tools for this are available in the `tourrr` package, too.

7. Acknowledgement

The article is created using Quarto [34] in R [13]. The source code for reproducing the work reported in this paper can be found at: <https://github.com/huizezhang-sherry/paper-jso>. Nicolas Langrené acknowledges the partial support of the Guangdong Provincial Key Laboratory IRADS (2022B1212010006, R0400001-22) and the UIC Start-up Research Fund UICR0700041-22.

References

- [1] J. B. Kruskal, Toward a practical method which helps uncover the structure of a set of observations by finding the line transformation which optimizes a new ‘index of condensation’, in: R. C. Milton, J. A. Nelder (Eds.), Statistical Computation, Academic Press, New York, 1969, pp. 427–440.
- [2] J. H. Friedman, J. W. Tukey, A Projection Pursuit Algorithm for Exploratory Data Analysis, IEEE Transactions on Computing C 23 (1974) 881–889.
- [3] P. Hall, On polynomial-based projection indices for exploratory projection pursuit, The Annals of Statistics 17 (1989) 589–605. URL: <https://doi.org/10.1214/aos/1176347127>.
- [4] D. Cook, A. Buja, J. Cabrera, Projection pursuit indexes based on orthonormal function expansions, Journal of Computational and Graphical Statistics 2 (1993) 225–250. URL: <https://doi.org/10.2307/1390644>.
- [5] E.-K. Lee, D. Cook, A projection pursuit index for large p small n data, Statistics and Computing 20 (2010) 381–392. URL: <https://doi.org/10.1007/s11222-009-9131-1>.
- [6] N. Loperfido, Skewness-based projection pursuit: A computational approach, Computational Statistics and Data Analysis 120 (2018) 42–57. doi:<https://doi.org/10.1016/j.csda.2017.11.001>.
- [7] N. Loperfido, Kurtosis-based projection pursuit for outlier detection in financial time series, The European Journal of Finance 26 (2020) 142–164. doi:<https://doi.org/10.1080/1351847X.2019.1647864>.
- [8] C. Posse, Projection pursuit exploratory data analysis, Computational Statistics & Data Analysis 20 (1995) 669–687. URL: <https://www.sciencedirect.com/science/article/pii/0167947395000028>. doi:[https://doi.org/10.1016/0167-9473\(95\)00002-8](https://doi.org/10.1016/0167-9473(95)00002-8).
- [9] S. L. Marie-Sainte, A. Berro, A. Ruiz-Gazen, An efficient optimization method for revealing local optima of projection pursuit indices, in: M. Dorigo, M. Birattari, G. A. Di Caro, R. Doursat, A. P. Engelbrecht, D. Floreano, L. M. Gambardella, R. Groß, E. Şahin, H. Sayama, T. Stützle (Eds.), Swarm Intelligence, Springer Berlin Heidelberg, Berlin, Heidelberg, 2010, pp. 60–71.
- [10] M. Grochowski, W. Duch, Fast projection pursuit based on quality of projected clusters, in: A. Dobnikar, U. Lotrič, B. Šter (Eds.), Adaptive and Natural Computing Algorithms, Springer Berlin Heidelberg, Berlin, Heidelberg, 2011, pp. 89–97.
- [11] D. Cook, A. Buja, J. Cabrera, C. Hurley, Grand tour and projection pursuit, Journal of Computational and Graphical Statistics 4 (1995) 155–172. URL: <https://doi.org/10.1080/10618600.1995.10474674>.

- [12] H. Wickham, D. Cook, H. Hofmann, A. Buja, tourr: An R package for exploring multivariate data with projections, *Journal of Statistical Software* 40 (2011) 1–18. URL: <http://doi.org/10.18637/jss.v040.i02>.
- [13] R Core Team, R: A Language and Environment for Statistical Computing, R Foundation for Statistical Computing, Vienna, Austria, 2023. URL: <https://www.R-project.org/>.
- [14] H. S. Zhang, D. Cook, U. Laa, N. Langrené, P. Menéndez, Visual diagnostics for constrained optimisation with application to guided tours, *The R Journal* 13 (2021) 624–641. doi:[10.32614/RJ-2021-105](https://doi.org/10.32614/RJ-2021-105).
- [15] J.-S. Chou, D.-N. Truong, A novel metaheuristic optimizer inspired by behavior of jellyfish in ocean, *Applied Mathematics and Computation* 389 (2021) 125535. doi:[10.1016/j.amc.2020.125535](https://doi.org/10.1016/j.amc.2020.125535).
- [16] K. Rajwar, K. Deep, S. Das, An exhaustive review of the metaheuristic algorithms for search and optimization: taxonomy, applications, and open challenges, *Artificial Intelligence Review* (2023) 1–71. doi:[10.1007/s10462-023-10470-y](https://doi.org/10.1007/s10462-023-10470-y).
- [17] P. Tukey, J. Tukey, Graphical display of data in three and higher dimensions, Wiley series in probability and mathematical statistics: Applied probability and statistics, Wiley, 1981. URL: <https://books.google.com.au/books?id=WBzvAAAAMAAJ>, in V. Barnett, *Interpreting multivariate data*.
- [18] U. Laa, D. Cook, Using tours to visually investigate properties of new projection pursuit indexes with application to problems in physics, *Computational Statistics* 35 (2020) 1171–1205. doi:[10.1007/s00180-020-00954-8](https://doi.org/10.1007/s00180-020-00954-8).
- [19] D. Bertsimas, J. Tsitsiklis, Simulated Annealing, *Statistical Science* 8 (1993) 10 – 15. URL: <https://doi.org/10.1214/ss/177011077>. doi:[10.1214/ss/1177011077](https://doi.org/10.1214/ss/1177011077).
- [20] C. Posse, Projection pursuit exploratory data analysis, *Computational Statistics and Data Analysis* 20 (1995) 669–687. URL: <https://www.sciencedirect.com/science/article/pii/016794739500028>. doi:[https://doi.org/10.1016/0167-9473\(95\)00002-8](https://doi.org/10.1016/0167-9473(95)00002-8).
- [21] E.-K. Lee, D. Cook, S. Klinke, T. Lumley, Projection pursuit for exploratory supervised classification, *Journal of Computational and Graphical Statistics* 14 (2005) 831–846. URL: <https://doi.org/10.1198/106186005X77702>.
- [22] K. Grimm, Kennzahlenbasierte Grafikauswahl, doctoral thesis, Universität Augsburg, 2016.
- [23] P. J. Huber, Projection pursuit, *Ann. Statist.* 13 (1985) 435–475. URL: <https://doi.org/10.1214/aos/1176349519>. doi:[10.1214/aos/1176349519](https://doi.org/10.1214/aos/1176349519).
- [24] A. B. Ursula Laa, Dianne Cook, G. Valencia, Hole or grain? a section pursuit index for finding hidden structure in multiple dimensions, *Journal of Computational and Graphical Statistics* 31 (2022) 739–752. URL: <https://doi.org/10.1080/10618600.2022.2035230>.
- [25] L. Wilkinson, A. Anand, R. Grossman, Graph-theoretic scagnostics, in: IEEE Symposium on Information Visualization, 2005. INFOVIS 2005., 2005, pp. 157–164. doi:[10.1109/INFVIS.2005.1532142](https://doi.org/10.1109/INFVIS.2005.1532142).
- [26] L. Wilkinson, G. Wills, Scagnostics distributions, *Journal of Computational and Graphical Statistics* 17 (2008) 473–491. URL: <https://doi.org/10.1198/106186008X320465>. doi:[10.1198/106186008X320465](https://doi.org/10.1198/106186008X320465). arXiv:<https://doi.org/10.1198/106186008X320465>.
- [27] R. Adams, J. Fournier, Sobolev spaces, volume 140 of *Pure and Applied Mathematics*, Elsevier, 2003.
- [28] E. Porcu, M. Bevilacqua, R. Schaback, C. Oates, The Matérn model: a journey through statistics, numerical analysis and machine learning, *Statistical Science* 39 (2024) 469–492.
- [29] DLMF, NIST Digital Library of Mathematical Functions, 2024. URL: <https://dlmf.nist.gov/10.25>, f. W. J. Olver, A. B. Olde Daalhuis, D. W. Lozier, B. I. Schneider, R. F. Boisvert, C. W. Clark, B. R. Miller, B. V. Saunders, H. S. Cohl, and M. A. McClain, eds.
- [30] C. E. Rasmussen, C. K. I. Williams, Gaussian processes for machine learning, The MIT Press, 2006.
- [31] T. Karvonen, Asymptotic bounds for smoothness parameter estimates in Gaussian process interpolation, *SIAM/ASA Journal on Uncertainty Quantification* 11 (2023) 1225–1257.
- [32] J. Guinness, M. Katzfuss, Y. Fahmy, GpGp: fast Gaussian process computation using Vecchia’s approximation, R package, 2021.
- [33] S. Abdulah, Y. Li, J. Cao, H. Ltaief, D. Keyes, M. Genton, Y. Sun, Large-scale environmental data science with Exa-GeoStatR, *Environmetrics* 34 (2023) e2770. doi:<https://doi.org/10.1002/env.2770>.
- [34] J. Allaire, C. Teague, C. Scheidegger, Y. Xie, C. Dervieux, Quarto, 2022. URL: <https://github.com/quarto-dev/quarto-cli>. doi:[10.5281/zenodo.5960048](https://doi.org/10.5281/zenodo.5960048).